Developmental Biology 422 (2017) 105–114

Contents lists available at ScienceDirect

Developmental Biology

journal homepage: www.elsevier.com/locate/developmentalbiology

Original research article

SPARC preserves follicular epithelium integrity in insect ovaries

Paula Irles[a,b], Saray Ramos[a], Maria-Dolors Piulachs[a,*]

[a] Institut de Biologia Evolutiva (CSIC-Universitat Pompeu Fabra), Passeig Marítim de la Barceloneta, 37, 08003 Barcelona, Spain
[b] Facultad de Agronomía e Ingeniería Forestal, Pontificia Universidad Católica de Chile, Av. Vicuña Mackenna 4860, Macul, Santiago de Chile, Chile

ABSTRACT

The importance of juvenile hormone regulating insect oogenesis suggests looking for genes whose expression is regulated by this hormone. SPARC is a calcium-binding glycoprotein that forms part of the extracellular membranes, which in vertebrates participates in bones mineralization or regulating cell proliferation in some cancer types. This large number of functions described for SPARC in different species might be related to the significant differences in its structure observed when comparing different species-groups. Indeed, these structural differences allow characterizing the different clades.

In the cockroach *Blattella germanica*, a SPARC homolog emerged from ovarian transcriptomes that were constructed to find genes responding to juvenile hormone. In insects, SPARC functions have been studied in oogenesis and in embryo development of *Drosophila melanogaster*. In the present work, using RNAi approaches, novel functions for SPARC in the *B. germanica* panoistic ovaries are described. We found that depletion of SPARC does not allow to the follicular cells to complete mitosis, resulting in giant follicular cells nuclei and in a great alteration of the ovarian follicle cytoskeleton.

The SPARC contribution to *B. germanica* oogenesis occurs stabilizing the follicular cell program and helping to maintain the nuclear divisions. Moreover, SPARC is necessary to maintain the cytoskeleton of the follicular cells. Any modification of these key processes disables females for oviposition.

1. Introduction

In insect ovarian follicles, the follicular epithelium is subject to changes during oogenesis. From the first steps of ovarian development, the follicular cells have a high rate of proliferation, arresting cytokinesis at the onset of vitellogenesis in the adult female, a process triggered by an increase of juvenile hormone (JH) titer in the hemolymph. However, JH not only induces vitellogenin transcription and release from the fat body (Coles, 1965; Comas et al., 2001; Valle et al., 1993), but also determines the patency in the follicular epithelium, which allows vitellogenin to reach the oocyte membrane (Abu-Hakima and Davey, 1977). When patency is fully active, the follicular cells contract and can lose up to 60% of their normal volume, thus leaving large intercellular spaces. The Na^+/K^+ ATPase pump, the main regulator of cell volume, is known to respond to JH and so it might be essential for patency (Abu-Hakima and Davey, 1979; Irles et al., 2013). Besides volume reduction, patency involves an important reorganization of the cytoskeleton and the junctional elements of follicular cells (Abu-Hakima and Davey, 1979; Huebner and Injeyan, 1981; Irles et al., 2013).

Among the proteins related to the changes of the follicular cell program, those involved in the reorganization of the cytoskeleton or associated with the basal lamina are candidates for regulation by JH. The analysis of *Blattella germanica* ovarian transcriptomes conducted in our laboratory to identify JH-dependent genes revealed that SPARC (secreted protein, acidic and rich in cysteine) may play a role in the regulation of the follicular cell changes described above. SPARC, also named BM40 and osteonectin, was first isolated from foetal calf bones by Termine and coworkers (Termine et al., 1981), and later cloned from endodermal cells in mouse embryo (Sage et al., 1984). It is a calcium-binding glycoprotein with multiple functions and it appears conserved from invertebrates to vertebrates (Martinek et al., 2002).

More functions have subsequently been attributed to SPARC in mammals, SPARC has been shown to play an important role in cell adhesion (including both, attachment and spreading) and has an influence in cellular processes that require new tissue formation, such as angiogenesis, tumorigenesis and tissue repair (Clark and Sage, 2008). In addition, the mechanisms of action of SPARC are complex and may lead to either apoptosis or cell proliferation depending on the cell environment and the process in which it participates (Nagaraju et al., 2014). SPARC also contributes to extracellular matrix functioning by mediating the activities of different growth factors (Bradshaw and Sage, 2001), plays an important role in cell-matrix interaction by

* Corresponding author.
E-mail address: mdolors.piulachs@ibe.upf-csic.es (M.-D. Piulachs).

http://dx.doi.org/10.1016/j.ydbio.2017.01.005
Received 3 August 2016; Received in revised form 23 December 2016; Accepted 5 January 2017
Available online 13 January 2017

preventing cell adhesion (Bradshaw et al., 2002, 2003; Brekken et al., 2003; Delany et al., 2003; Gilmour et al., 1998; Rotllant et al., 2008), and has a key function in mineralization and calcification of vertebrates bones (Kawasaki et al., 2007, 2004; Kawasaki and Weiss, 2006).

Numerous studies have explored the involvement of SPARC in the evolution of vertebrate tissue mineralization (Kawasaki et al., 2007; Torres-Nunez et al., 2015), establishing by phylogenetic analysis that the origin of SPARC took place *ca.* 480 million years ago, after the emergence of cartilaginous and bony fishes (Bertrand et al., 2013; Kawasaki et al., 2004). Bertrand and coworkers (Bertrand et al., 2013) proposed that genome duplication in the last common eumetazoan ancestor, resulted in different SPARC orthologs: the SPARC present in all eumetazoans, SPARCB present in some groups of deuterostomes, but absent in tetrapods (Bertrand et al., 2013), and SPARCL1 which is expressed in vertebrate skeletal cells (Kawasaki et al., 2004; Kawasaki and Weiss, 2006). All these SPARC orthologs differ in the general organization of the protein, with the larger differences observed in the acidic domain at the N-terminal end that changes in size and composition.

SPARC has been studied in a limited number of invertebrate species. In the cnidarian *Nematostella vectensis*, four SPARC orthologs have been identified, and none of them, contain the acidic domain I. Moreover, in early stages of development, their expression is restricted to the endoderm (Koehler et al., 2009). In the nematode *Caenorhabditis elegans*, SPARC is expressed in body wall muscles and gonads, while depletion of SPARC after RNAi treatment results in a reduced number of offspring, which then die as embryos or larvae (Fitzgerald and Schwarzbauer, 1998). Adult gonad or oocyte morphology did not appear to be altered after SPARC depletion, implying that the developmental defects observed in embryogenesis might derive from fertilization problems (Fitzgerald and Schwarzbauer, 1998). Among insects, SPARC has been thoroughly studied in *Drosophila melanogaster* with results revealing multiple functions in oogenesis and embryo development (Martinek et al., 2002), heart formation (Volk et al., 2014), cardiomyopathies (Hartley et al., 2016), as well as a protective role of “loser” cells from wing imaginal discs preventing them to entering into premature apoptosis (Portela et al., 2010). In *D. melanogaster* SPARC is essential for collagen IV assembly in the basal lamina, to maintain tissues integrity (Martinek et al., 2002).

In relation to insect oogenesis, Martinek and coworkers (Martinek et al., 2002) identified a SPARC homolog in *D. melanogaster* ovaries, with expression restricted to somatic cells. It was observed to accumulate in the basal pole of follicular cells and the basal lamina, with an increase of its expression during previtellogenic stages, indicating a SPARC contribution in oocyte development and vitellogenesis.

In the present work, based on the panoistic ovary of *B. germanica*, we show that SPARC has different roles in the follicular epithelium related to developmental stage of ovarian follicle. In last instar nymphs, SPARC appears to be involved in the activation of follicular cells proliferation, while in adults a new role is added, as SPARC participates in the regulation of the final steps of follicular cell program. Low levels of SPARC produce an increase of mitosis in a single cell, resulting in a dramatic growth of the nucleus that becomes multilobulate. Moreover, the distribution of F-actins microfilaments is highly altered, impeding egg oviposition. These SPARC functions are added to the large range of those previously described for the different SPARC orthologs that derive from the different structural characteristics of the SPARC proteins in the different clades, suggesting that new functions for this protein could appear.

2. Materials and methods

2.1. Animals and tissue sampling

Freshly ecdysed sixth instar nymphs and freshly ecdysed adult females of the cockroach *B. germanica* (L.) were obtained from a colony fed on Panlab dog chow and water *ad libitum*, kept in the dark at 29 ± 1 °C and 60–70% and relative humidity. The newly emerged adult females were maintained with males to ensure their having mated before their use in all experiments (the presence of spermatozoa in the spermathecae was assessed at the end of all experiments to confirm mating had occurred). Dissections and tissue sampling were performed on carbon dioxide-anaesthetized specimens, held under Ringer's saline. Nymphs and adults were examined at different ages (as shown in results section).

2.2. RNA extraction and expression studies

Total RNA was isolated using the GenElute Mammalian Total RNA kit (Sigma). An amount of 400 ng from each RNA extraction was DNAse treated (Promega, Madison, WI, USA) and reverse transcribed with Superscript II reverse transcriptase (Invitrogen, Carlsbad CA, USA) and random hexamers (Promega). RNA quantity and quality was estimated by spectrophotometric absorption at 260 nm/280 nm in a Nanodrop ND-1000® Spectrophotometer (NanoDrop Technologies, Wilmington, DE, USA).

Expression patterns for *B. germanica* SPARC (BgSPARC) were determined by quantitative RT-PCR (qRT-PCR) in ovaries from last instar nymphs and adults, during the first gonadotrophic cycle. PCR primers used in qRT-PCR expression studies were designed using Primer3 v.0.4.0 software (Rozen and Skaletsky, 2000), based on the cDNA of SPARC isolated from *B. germanica* ovarian EST libraries previously obtained in our laboratory (Irles et al., 2009b) and identified in the genome. The actin-5c gene of *B. germanica* was used as a reference for expression studies. PCR reactions were made using the SYBR Green Supermix (BioRad) containing 200 nM of each specific primer, and were run in triplicate. Amplification reactions were carried out at 95 °C for 2 min, and 40 cycles of 95 °C for 15 s and 60 °C for 30 s, using MyIQ Single Color RTPCR Detection System (BioRad). After the amplification phase, a dissociation curve was carried out to ensure that there was only one product (Irles et al., 2009a). Primer sequences used and the accession numbers of the sequences are shown in Table S1.

2.3. RNAi experiments

The cDNA of SPARC was isolated from *B. germanica* ovarian EST libraries previously obtained in our laboratory and identified in the genome. To knock-down BgSPARC and to assess the specificity of the phenotype, two dsRNAs (dsBgSPARC-1 and dsBgSPARC-2) were used. dsBgSPARC-1 was 419 bp in length corresponding to the region between nucleotides 356 and 1079. dsBgSPARC-2 was 302 bp in length corresponding to the region between nucleotides 1092 and 1394. A dsRNA (dsMock), corresponding to 180 bp of non-coding region of pSTBlue-I plasmid, was used as control. The dsRNA were synthesized in vitro as we previously described (Ciudad et al., 2006). The dose used was 1 μg of either dsBgSPARC or dsMock and was injected into newly emerged sixth nymphal instar females or in newly emerged adult females. Since the same ovary phenotype was observed either using dsBgSPARC-1 or dsSPARC-2, all RNAi treatments are hereafter referred to as dsBgSPARC.

The expression levels of SPARC transcript were assessed by qRT-PCR on 3-day-old and 8-day-old sixth nymphal instar females, and on 5-day-old and 7-day-old adult females.

2.4. Immunohistochemistry

Ovaries were dissected from the last instar nymphs and adults of different age. Fixing and staining were performed as previously described (Irles and Piulachs, 2014; Irles et al., 2013). The primary mouse antibody employed was E7: anti-β-tubulin (M. Klymkowsky,

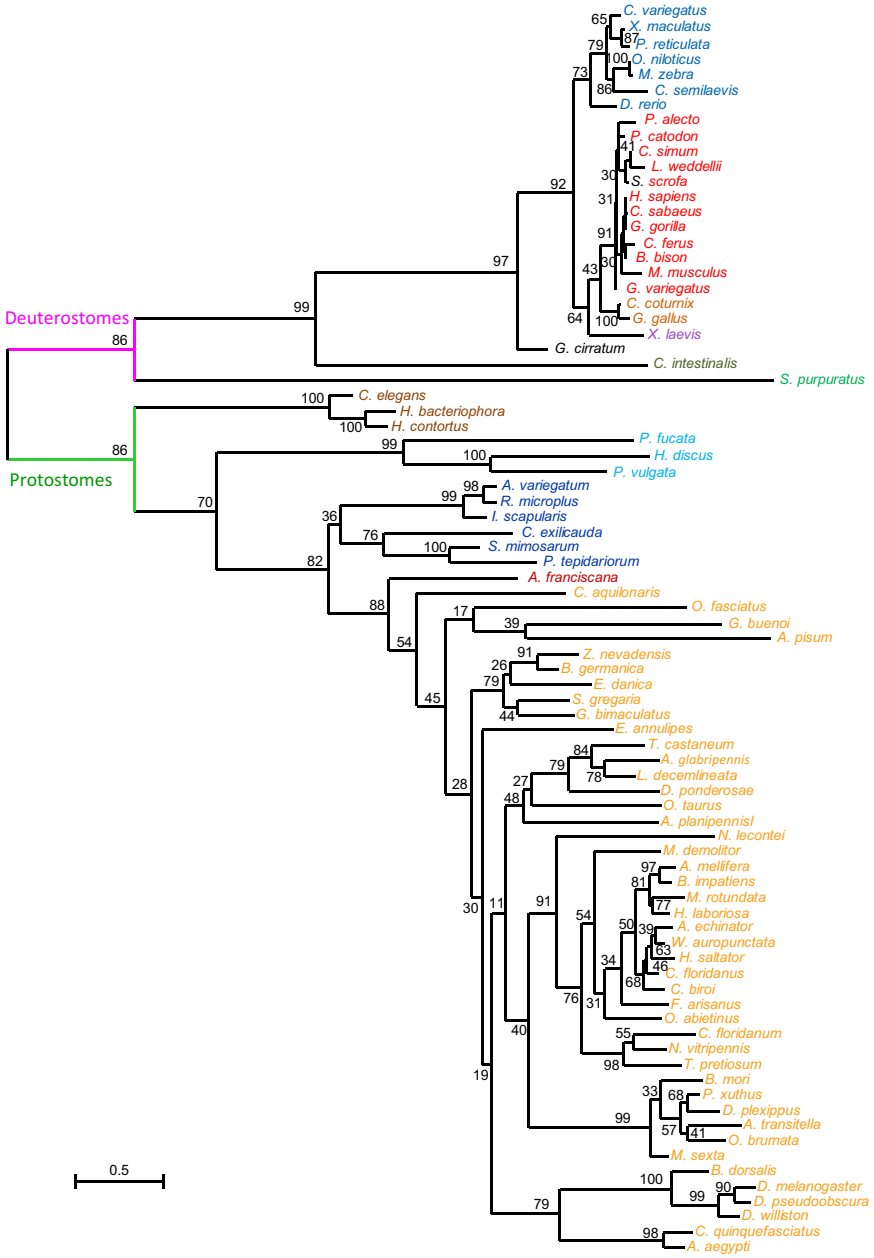

Fig. 1. Phylogenetic analysis of SPARC proteins. The analysis is based on the maximum-likelihood principle with the amino acid substitution model, and was carried out using SPARC sequences available in public databases. SPARC protein sequences were selected to cover all taxonomical groups of protostomes and deuterostomes. The complete species name and accession numbers of the sequences are indicated in Table S2. Species belonging to the same clade are highlighted with the same color. Scale bar indicates the number of substitutions per site.

Developmental Hybridoma Bank, USA) (diluted 1:50 in PBTBN). The primary rabbit antibodies used were anti-PH3 and anti-cleaved Caspase-3 (Asp175) (Cell Signaling Technology, Denver, MA, USA) (dilution 1:250). The samples were washed 3 times in PBTBN, left in PBTBN for 1 h and finally incubated with the secondary antibody Alexa-Fluor 488 goat anti-mouse or Alexa fluor 647 goat anti-rabbit, for 2 h. In addition ovaries were incubated at room temperature for 20 min in 300 ng/ml phalloidin-TRICT (Sigma) and then for 5 min in 1 µg/ml of DAPI (Sigma), for Actin-F and DNA staining, respectively. Tissues were mounted in Mowiol (Calbiochem, Madison, WI, USA) and observed using a Zeiss AxioImager.Z1microscope (Apotome) (Carl Zeiss MicroImaging).

The number of cells in the follicular epithelia was calculated following the procedure described by Pascual et al. (1992).

2.5. Juvenile hormone experiments

In vivo and in vitro experimental approaches were used to study the response of BgSPARC to JH, as described (Irles et al., 2013). First, the *corpora allata* from newly emerged adult females were removed (allatectomized females) in order to eliminate the endogenous JH (Piulachs et al., 2010). Three days later these allatectomized females were topically treated with 10 µg of JH III (Sigma) in 1 µl of acetone. Between 2 and 4 h post-treatment the ovaries were explanted and stored a −80 °C until use. Controls were equivalently treated with acetone.

The second approach involved an in vitro experiment using UM-BGE-1 cells derived from 4- to 5-day-old embryos of *B. germanica* (Kurtti and Brooks, 1977), which were maintained at 25 °C in Leibovitz-15 medium (Sigma, Madrid, Spain) supplemented as recommended by Munderloh and Kurtti (Munderloh and Kurtti, 1989). For

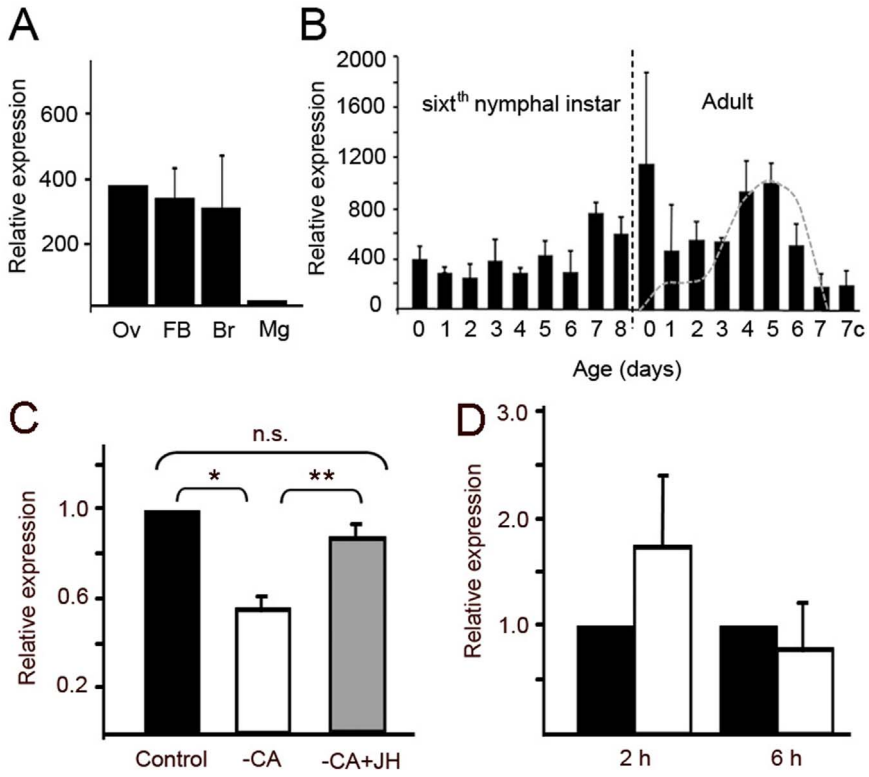

Fig. 2. Expression of BgSPARC in *Blattella germanica*. A. Relative expression of BgSPARC mRNA in ovaries (Ov), fat body (FB), brain (Br) and midgut (Mg) of adult female. B. Relative expression levels (qRT-PCR) of BgSPARC mRNA in the ovary from sixth instar nymphs and adults; the black dashed line indicates the moult to adult, the grey dashed line indicates the qualitative profile of JH levels in hemolymph of adult females (quantitative data is reported in Treiblmayr et al., 2006), and 7c corresponds to ovaries synthesizing the chorion.; in A and B data represent copies of mRNA per 1000 copies of BgActin-5c (relative expression), and are expressed as mean ± SEM (n=3). C. Effects of juvenile hormone (JH) on BgSPARC expression in ovaries. Newly emerged adult females were allatectomized (-CA), and a group treated with JH III (-CA +JH), 3 days later; the expression of BgSPARC was measured in ovaries between 2 and 4 h after treatment. BgSPARC expression in −CA is significantly reduced with respect to controls (* P(H1)=0.04), while the JH treatment (-CA+JH) significantly increased SPARC expression with respect to the −CA females (**(P(H1) =0.0001), reaching levels similar to those of control females. D. BgSPARC expression in *B. germanica* UM-BGE-1 cells treated with JH. The cells were incubated in the presence of JH III (10^{-6} M) for 2 and 6 h, and then harvested and processed to quantify the BgSPARC mRNA expression; control cells were incubated for the same period in an equivalent volume of acetone. Data represent normalized values against the controls (reference value =1), and are expressed as mean ± SEM (n=3).

JH III treatment, 10^6 cells/ml were seeded into 24-well cell-culture clusters (Costar, Amsterdam, The Netherlands) containing 10^{-6} M of JH III. Wells of control cells were added with the equivalent volume of acetone (1 ml). The cells were harvested 2 and 6 h post-treatment and kept at −80 °C until processing.

2.6. Phylogenetic studies

Sequences used in the phylogenetic analysis were obtained by Blast from GenBank, from i5k project (https://i5k.nal.usda.gov/webapp/blast/) (Poelchau et al., 2015), and from ASGARD database (http://asgard.rc.fas.harvard.edu/) (Ewen-Campen et al., 2011; Zeng et al., 2011), using the SPARC protein sequences from *B. germanica*, *D. melanogaster* and *T. castaneum* as query. The name of the species used and the corresponding accession numbers are listed in Table S2.

The complete amino acid sequences were aligned using the Mafft program with an iterative refinement method (E-INS-i) (Katoh and Standley, 2016). The resulting alignment was analysed by the RAxML program (Stamatakis et al., 2008) based on the maximum-likelihood principle, a JTT matrix, a gamma model of heterogeneity rate, and using empirical base frequencies and estimating proportions. The data was bootstrapped for 100 replicates.

The sequence domains were identified using the Conserved Domain Search Service (CD Search) from NCBI (Marchler-Bauer et al., 2015).

2.7. Statistical analysis

Quantitative data are described using the mean ± standard error of mean (SEM). To compare means of morphometric values the non-parametric Mann-Whitney test was used. Differences between expressions level were examined using the pair-wise fixed reallocation randomization test (performed using the Relative Expression Software Tool v.2.0.7; Corbett Research, Sydney, Australia). This test makes no assumptions regarding data distribution (Pfaffl et al., 2002).

3. Results

3.1. Blattella germanica *SPARC in the animal context*

The mRNA of *B. germanica* SPARC (BgSPARC) consisted of 1843 nucleotides, including the 5′ and 3′ untranslated regions, yielding an open reading frame of 960 nucleotides that codify for a protein of 320 amino acids, with a theoretical molecular weight of 37.4 kDa and an isoelectric point of 4.72.

The sequence of the BgSPARC protein is similar to other insect SPARC orthologs, showing 78% and 72% identity to the SPARC from the termite *Zootermopsis nevadensis* and the locust *Schistocerca gregaria*, respectively, but when compared with SPARC from the fly *D. melanogaster*, identity decreases to 44%.

As in other SPARC proteins, BgSPARC is structured in the three characteristic domains. Domain I is the most variable and consists of an acidic domain in the N-terminal end of the protein. Domain II, called the follistatin-like domain, is rich in cysteines and contains the

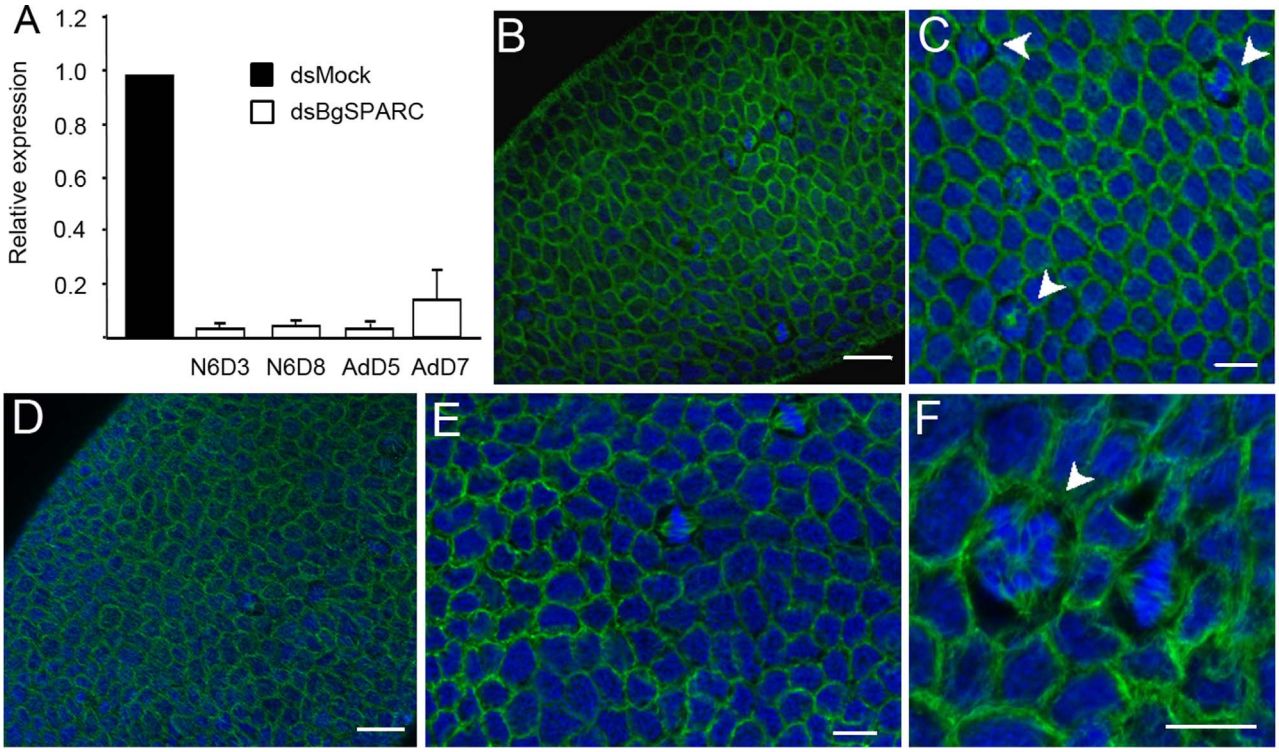

Fig. 3. BgSPARC in ovarian follicle development of *Blattella germanica*. A: Relative expression of BgSPARC in ovaries from females treated with dsBgSPARC at the first day of the sixth nymphal instar; BgSPARC levels were measured in 3-day-old (N6D3) and 8-day-old sixth instar nymphs (N6D8), and in 5-day-old (AdD5) and 7-day-old (AdD7) adults, showing that SPARC depletion continues through the first gonadotrophic cycle. Data represent normalized values against the controls (reference value=1), and are expressed as mean ± SEM (n=3–5). B-C: Follicular epithelium from 8-day-old dsMock-treated sixth instar nymph; mitotic figures are indicated by an arrowhead. D-F: Follicular epithelium from 8-day-old dsBgSPARC-treated sixth instar nymph; showing mitotic cells (E), and altered mitotic figures (F, arrowhead). Nuclei stained with DAPI appear in blue, whereas anti β-tubulin labelling appears in green. Scale bar in B, D: 20 μm, in C, E: 10 μm, and in F: 2 μm.

conserved putative N-glycosylation site. Domain III, which is located in the C-terminal end of the protein, is the extracellular calcium binding domain that contains an osteonectin-2 motif and an EF-hand calcium-binding domain (Fig. S1).

Although SPARC is generally conserved throughout the animal kingdom, the alignment of the sequences belonging to triploblastic organisms (Fig. S1) evidences two large blocks that separate the SPARC of deuterostomes from that of protostomes. In general, the SPARC sequences within a clade present a high level of mutual similarity. However, the comparison of SPARC protein sequences in both clades shows a clear divergence in the composition of the three domains (Fig. S1).

All deuterestome SPARC sequences contain 15 conserved cysteines (highlighted in red in Fig. S1) distributed along the protein, the first being located in the acidic domain, that are absent from the protostomes sequences. Moreover, the SPARC protein of all vertebrates contains one canonical Kazal-2 motif with three disulphide bonds in the follistatin domain, which is also conserved in the tunicate *Ciona intestinalis*, and also, although somewhat modified, in the sea urchin *Strongylocentrotus purpuratus*.

Within the protostomes, the SPARC protein sequence is also conserved in domains II and III. The amino acid composition of domain I is highly variable, but this variability declines when species belonging to the same clade are compared; then domain I appears less dissimilar. Across the class of insects, the degree of conservation of domain I is typical in the different orders (Fig. S1). In protostomes, the protein SPARC has 18 conserved cysteine residues (highlighted in red in Fig. S1). As indicated, they do not have any residues conserved in domain I but they do have two cysteine residues in the follistatin-like domain conserved in all the protostomes, as well as two more conserved cysteine residues in the extracellular calcium-binding domain. In total, there are four conserved cysteines that are not present in deuterostomes. In the protostomes, the Kazal-like motif experienced significant modification and can only be recognized with some degree of confidence in a few species, such as the Nematoda *Caenorhabditis elegans*, the Diptera *Bactrocera dorsalis* or the Araneae *Stegodyphus mimosarum*. Besides this modification in the Kazal motif, the three conserved disulphide bonds and the glycosylation site in follistatin-like domain are conserved in all protostomes.

Phylogenetic analysis in triploblastic organisms has shown that SPARC sequences differentiated early in evolution, producing two variants of the protein one for the deuterostomes (pink lines in Fig. 1) and one for the protostomes (green lines in Fig. 1). Among protostomes, all the species belonging to the same taxonomic class appear clustered with a high degree of consistency. The Nematoda and the Mollusca appeared as sister groups of Arthropoda, whereas the Arachnidae and the Crustacea, as expected, were the sister groups of Insecta. Between insects, in those orders with more than one representative, the species were also grouped.

The topology of the phylogenetic tree shows that SPARC has been modified according to the biological characteristics of each group. It is worth noting that branches are generally rather long, implying a notable degree of divergence, except in vertebrates, where the degree of conservation is remarkable. Of note, nurse shark (*Ginglymostoma cirratum*) SPARC is the sister group of all other vertebrate sequences, thus illustrating the change of SPARC function associated with bone mineralization in bony vertebrates.

3.2. *SPARC expression during* Blattella germanica *oogenesis*

BgSPARC is expressed in all adult female tissues analysed: ovaries, fat body, brain and midgut (Fig. 2A). In ovaries from sixth (last) nymphal instar and adult females in the first gonadotrophic cycle (Fig. 2B), BgSPARC mRNA levels start rising on 7-day-old sixth nymphal instar reaching a maximum at the day of emergency to adult.

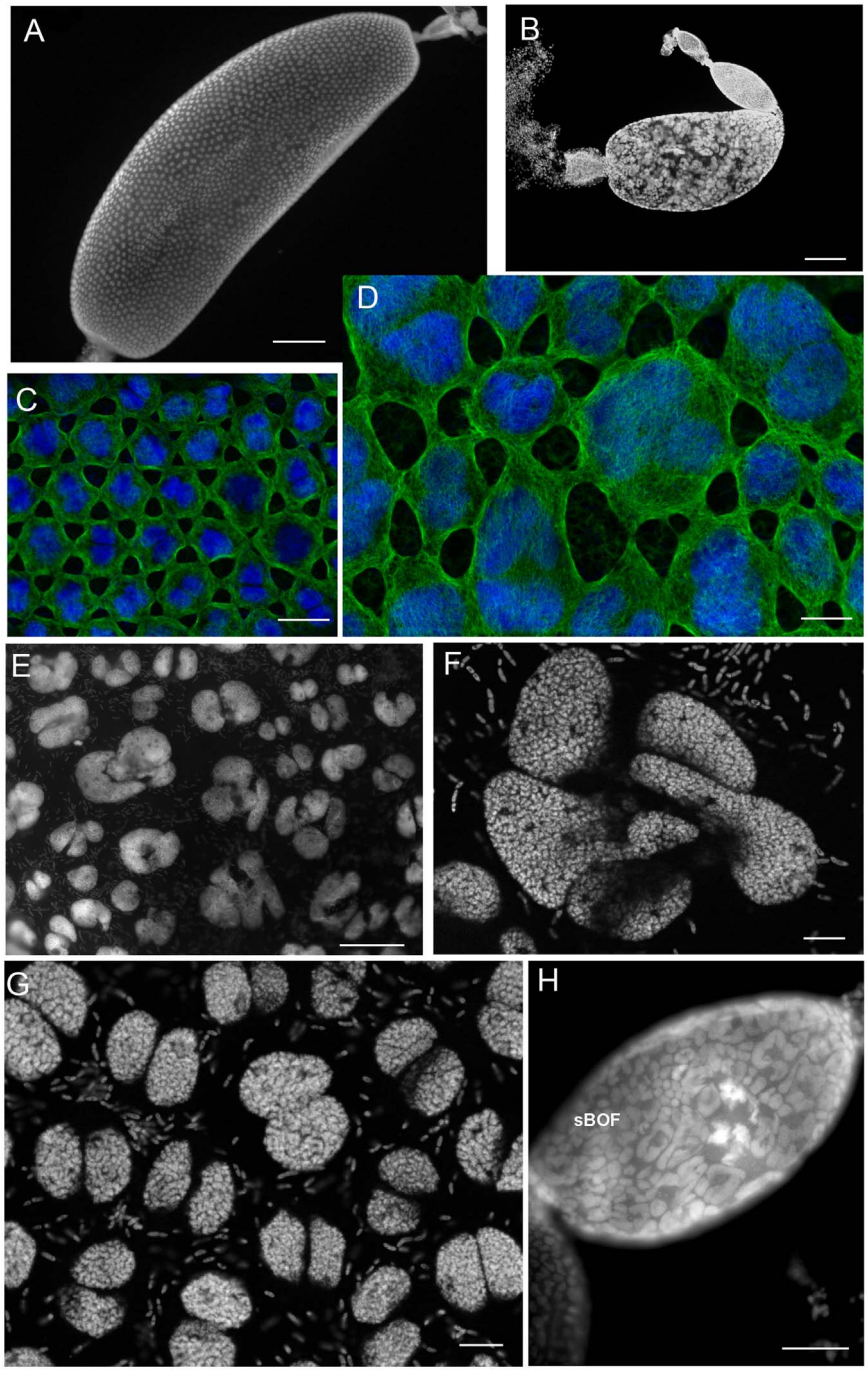

Fig. 4. SPARC depletion in 5-day-old adult *Blattella germanica* females previously treated with dsBgSPARC at the first day of the sixth nymphal instar. A: Basal ovarian follicle from a dsMock-treated adult female. B: Basal ovarian follicle from a profoundly affected dsBgSPARC-treated adult female showing the enlarged follicular cell nuclei. C: Follicular cells from a dsMock-treated adult female. D: Follicular cells from a dsBgSPARC-treated adult female; nuclei stained with DAPI appear in blue whereas β-tubulin labelling appears in green. E: Follicular cell nuclei in ovarian follicles from dsBgSPARC-treated adults. F: A follicular cell nucleus from a dsBgSPARC-treated adult. G: Nuclei from follicular cells in ovarian follicles from dsBgMock-treated adults. Comparing F and G reveals the differences in cell nucleus size observed among dsBgSPARC-treated females. In F and G there is clear evidence of stick-like endosymbiont bacteria around the DAPI stained nuclei. H: subbasal ovarian follicle (sBOF) from a dsBgSPARC-treated adult, showing the changes in nuclei morphology and size. Scale bar in A and B: 200 μm, in C and D: 20 μm, in E and H: 50 μm, and in F and G: 10 μm.

BgSPARC mRNA expression at the day of emergency was notably variable, suggesting a rapid modulation of its expression during the molting process. Later, in mid gonadotrophic cycle, BgSPARC mRNA expression show the highest average levels in ovaries from 4- and 5-day-old females. This high expression parallels the highest levels of JH in the hemolymph measured in the same days (Fig. 2B; Treiblmayr et al., 2006) and concurring with the patency process. The expression then rapidly decreases reaching a minimum in 7-day-old females, when the chorion synthesis takes place (Fig. 2B).

3.3. Effects of juvenile hormone on BgSPARC expression

The coincidence between high JH levels in the hemolymph and the high BgSPARC mRNA expression in ovaries during the gonadotrophic cycle, together with the presence of this mRNA in transcriptomes from individuals treated with JH III, suggested that the hormone directly or indirectly promotes BgSPARC expression. To test this hypothesis, newly emerged (0-day-old) adult females were allatectomized, and then, three days later, topically treated with 10 μg of JH III. The ovaries

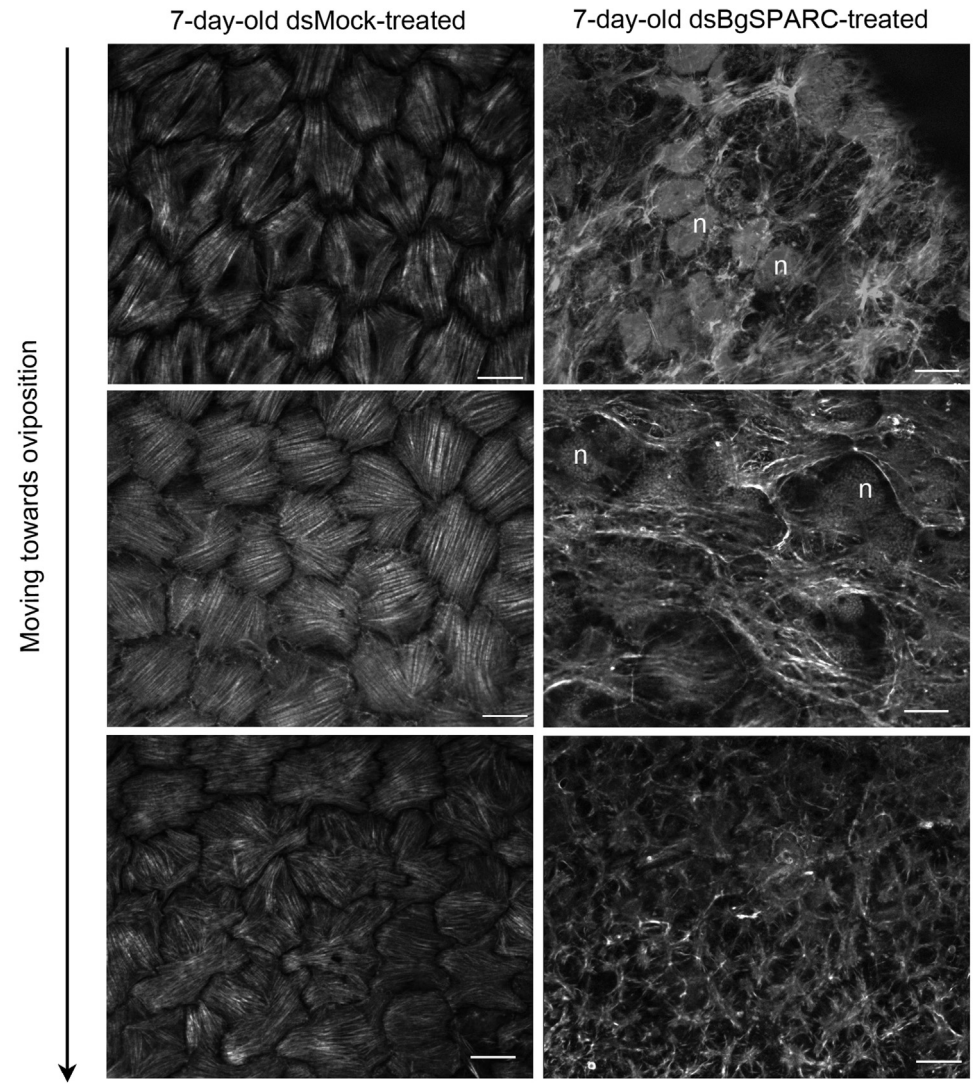

Fig. 5. Effect of BgSPARC depletion on cytoskeleton organization in the follicular cells of *Blattella germanica* ovarian follicles. The images show the changes in F-actin distribution in follicular cells from 7-day-old dsMock-treated and dsBgSPARC-treated adult females, as the ovarian follicle is moving to oviposition. In dsBgSPARC follicles some follicular cell nuclei (n) are still visible as they have not been completely covered by the F-actins. Scale bar: 20 μm. F-actin microfilaments were stained with phalloidin-TRITC, and nuclei with DAPI.

from these 3-day-old-treated females, and from the respective allatectomized controls, were dissected between 2 and 4 h after JH III application. BgSPARC mRNA levels were significantly reduced ($P(H1)=0.04$) in allatectomized control females, whereas the expression of BgSPARC significantly increased ($P(H1)=0.0001$) after JH treatment, reaching expression levels practically as those of non-allatectomized control females (Fig. 2C).

This influence of JH on BgSPARC expression was also studied in vitro, using *B. germanica* UM-BGE-1 cells incubated with JH III or acetone for 2 and 6 h. Two hours after adding JH III, the expression of BgSPARC in the embryonic cells tended to increase, although differences with respect to controls were not statistically significant. Then, 6 h after the JH III addition, the expression of BgSPARC became similar to that of control cells (Fig. 2D). These results suggest that JH enhanced the expression of BgSPARC and that this effect was transient.

3.4. Effects of BgSPARC depletion on oogenesis

In order to elucidate the function of BgSPARC in oocyte maturation, newly emerged sixth instar nymphs were treated with dsBgSPARC. BgSPARC mRNA levels were then measured in ovaries from 3-day-old and 8-day-old sixth instar nymphs. Expression was found to be 21-fold and 26-fold lower, respectively, in dsBgSPARC-treated with respect to dsMock-treated nymphs (Fig. 3A). BgSPARC depletion was maintained or even increased over the gonadotrophic cycle, showing 45-fold less expression in ovaries from 5-day-old dsBgSPARC-treated adults. Two days later, in 7-day-old adult females, the expression of BgSPARC tended to slightly recover (Fig. 3A). However, this tendency to recover at the end of the gonadotrophic cycle was insufficient to allow oviposition. Even-though the sponge-like body (the chorion structure where the micropile is located, which facilitates the embryo air-exchange) could be detected in most of the oocytes analysed (80%), a number of *B. germanica* chorion-related genes were not expressed (Fig. S2). Only 8% of dsBgSPARC-treated females (n=25) formed a proper ootheca, and only 60% of the nymphs hatched from these oothecae. Non-oviposited oocytes retained in the ovary were not resorbed, appearing as aggregated masses, which suggest that these oocytes were unable to undergo apoptosis or reabsorption processes (Fig. S3).

During *B. germanica* oogenesis, the follicular epithelium from basal ovarian follicles must reach an optimal cell number to cover the growing oocyte and ensure oogenesis completion. This occurs during the last nymphal instar and the first days of adulthood (previtellogenic period), when the follicular epithelium is mitotically active (Fig. 3B and C; and S4A). Although the number of mitotic cells was not significantly affected in basal ovarian follicles of 8-day-old

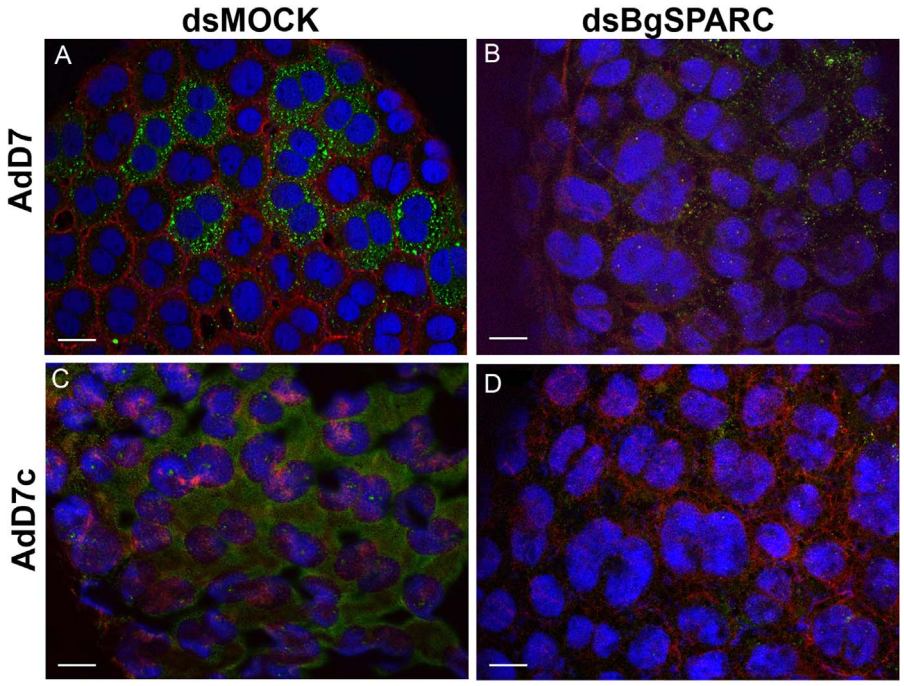

Fig. 6. Cell death in the follicular epithelium of BgSPARC-treated females at the end of the first gonadotrophic cycle. Labelling for cleaved caspase-3 (green) in the basal ovarian follicle from 7-day-old dsMock (A) and dsBgSPARC (B) treated females; and in chorionated 7-day-old dsMock (C) and dsBgSPARC (D) treated females (7c). F-actin microfilaments (red) were stained with phalloidin-TRITC, and nuclei with DAPI (blue). Scale bars 20 μm.

sixth nymphal instar (Fig. 3D–F and S4B), the total number of follicular cells decreased. Thus, we observed 3164 ± 100 cells in the follicular epithelium of BgdsSPARC-treated nymphs, while there were typically 3665 ± 144 in dsMock-treated nymphs (P=0.008). In addition, β-tubulin labelling revealed that most of the cells undergoing division had poorly orientated and disproportionate numbers of mitotic spindles (Fig. 3F, arrow).

Later, in 5-day-old dsBgSPARC-treated adult females, the basal ovarian follicles were smaller (1.14 ± 0.16 mm in length) than in dsMock-treated females (1.54 ± 0.11 mm; Fig. 4A and B). This delay in growing was not due to a failure of vitellogenin expression in fat body from treated females, since vitellogenin expression increased in comparison to dsMock treated females (Fig. S5). Moreover, most of the basal ovarian follicles in these dsBgSPARC-treated females were pear-shaped and showed a fragile aspect. The follicular cells had a remarkable shape variation, and a great variability in size, most of them being bigger than those of dsMock-treated ovarian follicles (Fig. 4C and D), displaying large multilobulate nuclei (Fig. 4E and F, compared to G) with complex morphologies (Fig. 4F). Furthermore, the effects of BgSPARC depletion were not limited to the basal ovarian follicles (being the only ones that develop in each gonadotrophic cycle); these features of the follicular cells were also observed in the epithelium of subbasal ovarian follicles, which presented big cells with giant nuclei (Fig. 4H).

Moreover, at the end of the gonadotrophic cycle, the cytoskeleton was dramatically modified (Fig. 5). The actins, which facilitate follicle contractions when expelling the egg, were observed to form largely disorganized fibres covering the follicle (Fig. 5). Additionally, as showed by the absence of Caspase-3 immunostaining (Fig. 6), the follicular cells of dsBgSPARC-treated females did not enter in apoptosis, a process that facilitates the disengaging of follicular cells from the chorion, and the release of the egg. As a consequence of all these changes, most of the dsBgSPARC-treated females were unable to oviposit at the end of the gonadotrophic cycle.

4. Discussion

Some of the functions attributed to SPARC seem contradictory. This is because the protein has different roles depending on the tissue and the cell type (Nagaraju et al., 2014). SPARC has been thoroughly studied regarding vertebrate bone mineralization, but the objective of most studies was to understand its role in different types of cancer cell, where it may have anti-proliferative properties (Nagaraju and Sharma, 2011). In general, the SPARC functions take place in tissues that are remodeled during development (Koehler et al., 2009; Portela et al., 2010; Shahab et al., 2015).

According to our phylogenetic analysis, the wide range of functions attributed to SPARC can be explained by the different structure of the protein in the different animal species. Although there are significant variations, the structure of SPARC proteins is generally conserved across species in the same clade; hence the clade can be characterized according to this structure, for example, in the case of insects belonging to the same order.

We expected to observe generalized defects during metamorphosis due to the SPARC relation with extracellular membranes (Bassuk et al., 2000; Shahab et al., 2015). BgSPARC-depleted females, however, molted correctly, they had no motility problems, had the fat body active producing vitellogenin, and did not show problems of gut motility that might impair food uptake. Interestingly, SPARC has been localized in the ovary of *D. melanogaster* (Martinek et al., 2002). This suggests that the functions described herein could also operate in this fly species. Our experiments showed that BgSPARC depletion results in an uncontrolled growth of follicular cell nucleus, which did not enter in apoptosis and, in general, there was a disorganization of the ovarian follicles cytoskeleton; alterations that were so dramatic that prevented oviposition.

The phenotypes observed in *B. germanica* ovaries appear to correspond to the combination of different SPARC functions, which are sequential in time and may be differentially regulated. The reduction in the number of follicular cells was the first phenotype observed after dsBgSPARC treatment and this occurs during the last nymphal instar. The implication of SPARC in cell proliferation was not

surprising as this role has been described in different cell types, including a number of different cancer types, whether inhibiting or stimulating proliferation (Bassuk et al., 2000; Bhoopathi et al., 2012; Chen et al., 2012). Moreover, while our results suggest that JH promotes BgSPARC expression (Fig. 2C) in adults, it is clear that BgSPARC can also be expressed in the absence of JH as this hormone is not produced in the last nymphal instar (Treiblmayr et al., 2006) when SPARC plays a role in follicular cells.

Later, in adults, the phenotypes produced by SPARC depletion are stressed. In ovaries from adult *B. germanica*, the correct evolution of the follicular cell program means that they should become binucleated when cytokinesis is arrested during the vitellogenesis period, coinciding with the higher levels of JH in the hemolymph (Treiblmayr et al., 2006). Most of the follicular cells from dsBgSPARC-treated females, presented enlarged multilobulate nucleus, possibly due to the unusual number of asymmetric and multipolar mitosis that result in an accumulation of chromatin. This finding is reminiscent of the process occurring in some cancer cells which accumulate highly variable quantities of DNA in their nuclei (see Pihan, 2013). In dsBgSPARC-treated females, the changes produced in the cytoskeleton apparently determined modifications in the morphology of basal ovarian follicles, which appear rounded, as observed in *D. melanogaster*, where SPARC is associated with the basal lamina (Isabella and Horne-Badovinac, 2015).

We have shown that BgSPARC depletion does not determine a reduction of vitellogenin expression. As vitellogenin is a strictly JH-dependent gene (Cruz et al., 2003), we can presume that JH production in these dsBgSPARC-treated females was not affected. This and the other lines of evidence suggest that JH promotes BgSPARC expression during the gonadotrophic cycle, whereas, in turn, BgSPARC contributes to oogenesis in panoistic ovaries by stabilizing the follicular cells program, helping to maintain the nuclear division and the cytoskeleton organization.

Author contributions

PI and SR performed the laboratory work; PI and MDP conceived, designed and drafted the manuscript. MDP obtained the necessary funding. The authors gave their final approval for publication.

Acknowledgments

Thanks are due to Xavier Belles for fruitful discussions on the results and on the manuscript. We also thank the financial support from the Ministry of Science and Innovation, Spain (Grant number BFU2011-22404), and from the Catalan Regional Government (Grant 2014 SGR 619). PI is the recipient of a postdoctoral research grant (BECAS CHILE from CONICYT, Chile (74110076) and the Apoyo al Retorno de Investigadores desde el Extranjero Program [*Convocatoria* 2013, 821320046, PAI, CONICYT]). The funders had no role in the design of the study, data collection or analysis, the decision to publish, or in the preparation of the manuscript.

Appendix A. Supporting information

Supplementary data associated with this article can be found in the online version at doi:10.1016/j.ydbio.2017.01.005.

References

Abu-Hakima, R., Davey, K.G., 1977. The action of juvenile hormone on follicle cells of Rhodnius prolixus in vitro: the effect of colchicine and cytochalasin B. Gen. Comp. Endocrinol. 32, 360–370.

Abu-Hakima, R., Davey, K.G., 1979. A possible relationship between ouabain-sensitive (Na+-K+) dependent ATPase and the effect of juvenile hormone on the follicle cells of Rhodnius prolixus. Insect Biochem. 9, 195–198.

Bassuk, J.A., Pichler, R., Rothmier, J.D., Pippen, J., Gordon, K., Meek, R.L., Bradshaw, A.D., Lombardi, D., Strandjord, T.P., Reed, M., Sage, E.H., Couser, W.G., Johnson, R., 2000. Induction of TGF-beta1 by the matricellular protein SPARC in a rat model of glomerulonephritis. Kidney Int. 57, 117–128.

Bertrand, S., Fuentealba, J., Aze, A., Hudson, C., Yasuo, H., Torrejon, M., Escriva, H., Marcellini, S., 2013. A dynamic history of gene duplications and losses characterizes the evolution of the SPARC family in eumetazoans. In: Proceedings of the Biological sciences/The Royal Society, vol. 280, 20122963.

Bhoopathi, P., Gorantla, B., Sailaja, G.S., Gondi, C.S., Gujrati, M., Klopfenstein, J.D., Rao, J.S., 2012. SPARC overexpression inhibits cell proliferation in neuroblastoma and is partly mediated by tumor suppressor protein PTEN and AKT. PLoS One 7, e36093.

Bradshaw, A.D., Sage, E.H., 2001. SPARC, a matricellular protein that functions in cellular differentiation and tissue response to injury. J. Clin. Investig. 107, 1049–1054.

Bradshaw, A.D., Reed, M.J., Sage, E.H., 2002. SPARC-null mice exhibit accelerated cutaneous wound closure. J. Histochem. Cytochem. 50, 1–10.

Bradshaw, A.D., Puolakkainen, P., Dasgupta, J., Davidson, J.M., Wight, T.N., Helene Sage, E., 2003. SPARC-null mice display abnormalities in the dermis characterized by decreased collagen fibril diameter and reduced tensile strength. J. Investig. Dermatol. 120, 949–955.

Brekken, R.A., Puolakkainen, P., Graves, D.C., Workman, G., Lubkin, S.R., Sage, E.H., 2003. Enhanced growth of tumors in SPARC null mice is associated with changes in the ECM. J. Clin. Investig. 111, 487–495.

Chen, J., Wang, M., Xi, B., Xue, J., He, D., Zhang, J., Zhao, Y., 2012. SPARC is a key regulator of proliferation, apoptosis and invasion in human ovarian cancer. PLoS One 7, e42413.

Ciudad, L., Piulachs, M.D., Belles, X., 2006. Systemic RNAi of the cockroach vitellogenin receptor results in a phenotype similar to that of the Drosophila yolkless mutant. FEBS J. 273, 325–335.

Clark, C.J., Sage, E.H., 2008. A prototypic matricellular protein in the tumor microenvironment–where there's SPARC, there's fire. J. Cell Biochem 104, 721–732.

Coles, G.C., 1965. Studies on the hormonal control of metabolism in Rhodnius prolixus Stål—I. The adult female. J. Insect Physiol. 11, 1325–1330.

Comas, D., Piulachs, M.D., Belles, X., 2001. Induction of vitellogenin gene transcription in vitro by juvenile hormone in Blattella germanica. Mol. Cell. Endocrinol. 183, 93–100.

Cruz, J., Martin, D., Pascual, N., Maestro, J.L., Piulachs, M.D., Belles, X., 2003. Quantity does matter. Juvenile hormone and the onset of vitellogenesis in the German cockroach. Insect Biochem. Mol. Biol. 33, 1219–1225.

Delany, A.M., Kalajzic, I., Bradshaw, A.D., Sage, E.H., Canalis, E., 2003. Osteonectin-null mutation compromises osteoblast formation, maturation, and survival. Endocrinology 144, 2588–2596.

Ewen-Campen, B., Shaner, N., Panfilio, K.A., Suzuki, Y., Roth, S., Extavour, C.G., 2011. The maternal and early embryonic transcriptome of the milkweed bug Oncopeltus fasciatus. BMC Genom. 12, 61.

Fitzgerald, M.C., Schwarzbauer, J.E., 1998. Importance of the basement membrane protein SPARC for viability and fertility in Caenorhabditis elegans. Curr. Biol. 8, 1285–1288.

Gilmour, D.T., Lyon, G.J., Carlton, M.B., Sanes, J.R., Cunningham, J.M., Anderson, J.R., Hogan, B.L., Evans, M.J., Colledge, W.H., 1998. Mice deficient for the secreted glycoprotein SPARC/osteonectin/BM40 develop normally but show severe age-onset cataract formation and disruption of the lens. EMBO J. 17, 1860–1870.

Hartley, P.S., Motamedchaboki, K., Bodmer, R., Ocorr, K., 2016. SPARC-Dependent Cardiomyopathy in Drosophila. Circ. Cardiovasc. Genet. 9, 119–129.

Huebner, E., Injeyan, H., 1981. Follicular modulation during oocyte development in an insect: formation and modification of septate and gap junctions. Dev. Biol. 83, 101–113.

Irles, P., Piulachs, M.D., 2014. Unlike in Drosophila Meroistic Ovaries, hippo represses notch in Blattella germanica Panoistic ovaries, triggering the mitosis-endocycle switch in the follicular cells. PLoS One 9, e113850.

Irles, P., Belles, X., Piulachs, M.D., 2009a. Brownie, a gene involved in building complex respiratory devices in insect eggshells. PLoS One 4, e8353.

Irles, P., Belles, X., Piulachs, M.D., 2009b. Identifying genes related to choriogenesis in insect panoistic ovaries by Suppression Subtractive Hybridization. BMC Genom. 10, 206.

Irles, P., Silva-Torres, F.A., Piulachs, M.D., 2013. RNAi reveals the key role of Nervana 1 in cockroach oogenesis and embryo development. Insect Biochem. Mol. Biol. 43, 178–188.

Isabella, A.J., Horne-Badovinac, S., 2015. Dynamic regulation of basement membrane protein levels promotes egg chamber elongation in Drosophila. Dev. Biol. 406, 212–221.

Katoh, K., Standley, D., 2016. A simple method to control over-alignment in the MAFFT multiple sequence alignment program. Bioinformatics.

Kawasaki, K., Weiss, K.M., 2006. Evolutionary genetics of vertebrate tissue mineralization: the origin and evolution of the secretory calcium-binding phosphoprotein family. J. Exp. Zool. B Mol. Dev. Evol. 306, 295–316.

Kawasaki, K., Suzuki, T., Weiss, K.M., 2004. Genetic basis for the evolution of vertebrate mineralized tissue. Proc. Natl. Acad. Sci. USA 101, 11356–11361.

Kawasaki, K., Buchanan, A.V., Weiss, K.M., 2007. Gene duplication and the evolution of vertebrate skeletal mineralization. Cells Tissues Organs 186, 7–24.

Koehler, A., Desser, S., Chang, B., MacDonald, J., Tepass, U., Ringuette, M., 2009. Molecular evolution of SPARC: absence of the acidic module and expression in the endoderm of the starlet sea anemone, Nematostella vectensis. Dev. Genes Evol. 219, 509–521.

Kurtti, T.J., Brooks, M.A., 1977. Isolation of cell lines from embryos of the cockroach, Blattella germanica. In vitro 13, 11–17.

Marchler-Bauer, A., Derbyshire, M.K., Gonzales, N.R., Lu, S., Chitsaz, F., Geer, L.Y., Geer, R.C., He, J., Gwadz, M., Hurwitz, D.I., Lanczycki, C.J., Lu, F., Marchler, G.H., Song, J.S., Thanki, N., Wang, Z., Yamashita, R.A., Zhang, D., Zheng, C., Bryant, S.H., 2015. CDD: NCBI's conserved domain database. Nucleic Acids Res. 43, D222–D226.

Martinek, N., Zou, R., Berg, M., Sodek, J., Ringuette, M., 2002. Evolutionary conservation and association of SPARC with the basal lamina in Drosophila. Dev. Genes Evol. 212, 124–133.

Munderloh, U.G., Kurtti, T.J., 1989. Formulation of medium for tick cell culture. Exp. Appl. Acarol. 7, 219–229.

Nagaraju, G.P., Sharma, D., 2011. Anti-cancer role of SPARC, an inhibitor of adipogenesis. Cancer Treat. Rev. 37, 559–566.

Nagaraju, G.P., Dontula, R., El-Rayes, B.F., Lakka, S.S., 2014. Molecular mechanisms underlying the divergent roles of SPARC in human carcinogenesis. Carcinogenesis 35, 967–973.

Pascual, N., Cerdá, X., Benito, B., Tomás, J., Piulachs, M.D., Belles, X., 1992. Ovarian ecdysteroid levels and basal oöcyte development during maturation in the cockroach *Blattella germanica* (L.). J. Insect Physiol. 38, 339–348.

Pfaffl, M.W., Horgan, G.W., Dempfle, L., 2002. Relative expression software tool (REST) for group-wise comparison and statistical analysis of relative expression results in real-time PCR. Nucleic Acids Res. 30, e36.

Pihan, G.A., 2013. Centrosome dysfunction contributes to chromosome instability, chromoanagenesis, and genome reprograming in cancer. Front. Oncol. 3, 277.

Piulachs, M.D., Pagone, V., Belles, X., 2010. Key roles of the Broad-Complex gene in insect embryogenesis. Insect Biochem. Mol. Biol. 40, 468–475.

Poelchau, M., Childers, C., Moore, G., Tsavatapalli, V., Evans, J., Lee, C.Y., Lin, H., Lin, J.W., Hackett, K., 2015. The i5k Workspace@NAL–enabling genomic data access, visualization and curation of arthropod genomes. Nucleic Acids Res. 43, D714–D719.

Portela, M., Casas-Tinto, S., Rhiner, C., Lopez-Gay, J.M., Dominguez, O., Soldini, D., Moreno, E., 2010. Drosophila SPARC is a self-protective signal expressed by loser cells during cell competition. Dev. Cell 19, 562–573.

Rotllant, J., Liu, D., Yan, Y.L., Postlethwait, J.H., Westerfield, M., Du, S.J., 2008. Sparc (Osteonectin) functions in morphogenesis of the pharyngeal skeleton and inner ear. Matrix Biol. 27, 561–572.

Rozen, S., Skaletsky, H., 2000. Primer3 on the www for general users and for biologist programmers. Methods Mol. Biol. 132, 365–386.

Sage, H., Johnson, C., Bornstein, P., 1984. Characterization of a novel serum albumin-binding glycoprotein secreted by endothelial cells in culture. J. Biol. Chem. 259, 3993–4007.

Shahab, J., Baratta, C., Scuric, B., Godt, D., Venken, K.J., Ringuette, M.J., 2015. Loss of SPARC dysregulates basal lamina assembly to disrupt larval fat body homeostasis in Drosophila melanogaster. Dev. Dyn. 244, 540–552.

Stamatakis, A., Hoover, P., Rougemont, J., 2008. A rapid bootstrap algorithm for the RAxML web-servers. Syst. Biol. 75, 758–771.

Termine, J.D., Belcourt, A.B., Conn, K.M., Kleinman, H.K., 1981. Mineral and collagen-binding proteins of fetal calf bone. J. Biol. Chem. 256, 10403–10408.

Torres-Nunez, E., Suarez-Bregua, P., Cal, L., Cal, R., Cerda-Reverter, J.M., Rotllant, J., 2015. Molecular cloning and characterization of the matricellular protein Sparc/osteonectin in flatfish, Scophthalmus maximus, and its developmental stage-dependent transcriptional regulation during metamorphosis. Gene 568, 129–139.

Treiblmayr, K., Pascual, N., Piulachs, M.D., Keller, T., Belles, X., 2006. Juvenile hormone titer versus juvenile hormone synthesis in female nymphs and adults of the German cockroach, Blattella germanica. J. Insect Sci. 6, 1–7.

Valle, D., Kun, J., Linss, J., Garcia Ede, S., Goldenberg, S., 1993. cDNA cloning and expression of Rhodnius prolixus vitellogenin. Insect Biochem. Mol. Biol. 23, 457–465.

Volk, T., Wang, S., Rotstein, B., Paululat, A., 2014. Matricellular proteins in development: perspectives from the Drosophila heart. Matrix Biol. 37, 162–166.

Zeng, V., Villanueva, K.E., Ewen-Campen, B.S., Alwes, F., Browne, W.E., Extavour, C.G., 2011. De novo assembly and characterization of a maternal and developmental transcriptome for the emerging model crustacean Parhyale hawaiensis. BMC Genom. 12, 581.